

Article

Research on Intelligent Identification Algorithm for Steel Wire Rope Damage Based on Residual Network

Jialin Han, Yiqing Zhang , Zesen Feng and Ling Zhao

College of Mechanical and Automotive Engineering, Liaocheng University, Liaocheng 252000, China; 13583002558@163.com (J.H.); feng_zesen99@163.com (Z.F.); zhaoling@lcu.edu.cn (L.Z.)

* Correspondence: yiqingzhang@lcu.edu.cn

Abstract: As a load-bearing tool, steel wire rope plays an important role in industrial production. Therefore, diagnosing the fracture and damage of steel wire ropes is of great significance for ensuring their safe operation. However, the detection and identification of wire rope breakage damage mainly focus on identifying external damage characteristics, while research on inspecting internal breakage damage is still relatively limited. To address the challenge, an intelligent detecting method is proposed in this paper for diagnosing internal wire breakage damage, and it introduces residual modules to enhance the network's feature extraction ability. Firstly, time–frequency analysis techniques are used to convert the extracted one-dimensional magnetic flux leakage (MFL) signal into a two-dimensional time–frequency map. Secondly, the focus of this article is on constructing a residual network to identify the internal damage accurately with the features of the time–frequency map of the MFL signal being automatically extracted. Finally, the effectiveness of the proposed method in identifying broken wires is verified through comparative experiments on detecting broken wires in steel wire ropes. Three common recognition methods, the backpropagation (BP) neural network, the support vector machine (SVM), and the convolutional neural network (CNN), are used as comparisons. The experimental results show that the residual network recognition method can effectively identify internal and external wire breakage faults in steel wire ropes, which is of great significance for achieving quantitative detection of steel wire ropes.

Keywords: steel wire rope; residual network; quantitative identification



Citation: Han, J.; Zhang, Y.; Feng, Z.; Zhao, L. Research on Intelligent Identification Algorithm for Steel Wire Rope Damage Based on Residual Network. *Appl. Sci.* **2024**, *14*, 3753. <https://doi.org/10.3390/app14093753>

Academic Editor: Mickaël Lallart

Received: 29 March 2024

Revised: 25 April 2024

Accepted: 26 April 2024

Published: 28 April 2024



Copyright: © 2024 by the authors. Licensee MDPI, Basel, Switzerland. This article is an open access article distributed under the terms and conditions of the Creative Commons Attribution (CC BY) license (<https://creativecommons.org/licenses/by/4.0/>).

1. Introduction

As one of the important load-bearing tools in industrial production, steel wire ropes have the advantages of high strength and stable and reliable use and have important applications in engineering fields such as coal mines, offshore oil development, and bridge traction [1–3]. However, due to prolonged exposure to harsh working environments and long-term high-load conditions, steel wire ropes inevitably suffer from various damages such as wire breakage, wear, and corrosion, which emphasizes the need for effective monitoring and maintenance methods. Unfortunately, the timely evaluation of the safety status of in-service wire ropes is hindered by the lack of effective wire rope damage detection methods and rigorous safety assessment techniques [4,5]. This leads to potential safety hazards going undetected. Hence, there exists an urgent imperative to cultivate a scientifically robust quantitative identification methodology for detecting broken wires. Such an approach would not only yield economic advantages but also harbor substantial societal significance. Therefore, developing a scientifically effective quantitative identification method for broken wires has high economic benefits and social value.

At present, the detection technology for steel wire ropes mainly includes destructive testing and non-destructive testing. Destructive testing may cause damage to the steel wire rope due to the need for tensile or fatigue testing, so non-destructive testing technology has been widely applied. The commonly used non-destructive testing methods currently

include ultrasonic testing [6], thermal imaging testing [7], infrared testing, and electromagnetic testing [8]. Due to its simple principle and high reliability, the electromagnetic detection method is highly suitable for the detection of damage in steel wire ropes with good magnetic conductivity [9].

In recent years, in order to accurately and quantitatively evaluate the defect information of steel wire ropes, experts and scholars have proposed various signal processing and fault recognition technologies. The initial signal of detected wire breakage from sensors typically involves a significant amount of noise [10]. To distill the distinctive features of the damaged signal, preprocessing of the signal is essential [11]. Ju Won Kim et al. use an envelope process based on Hilbert transform to reduce noise and improve the resolution of magnetic flux leakage (MFL) signals [12]. Mukhopadhyay et al. use wavelet transform decomposition and reconstruction techniques to denoise the original damage signal [13].

Early quantitative recognition primarily relies on the manual extraction of signal features, which are used to form feature vectors based on extracted characteristics such as peak, width, and peak-to-peak. The feature vectors are then fed into the network for training, ultimately allowing the classification and recognition of broken wires to be enabled. Qin et al., who used a wavelet decomposition and reconstruction algorithm to process magnetic leakage signals, designed an SVM classifier and achieved quantitative identification of broken wires, thereby proving the effectiveness of SVM classification [14]. Zhou et al. proposed a time–frequency domain coupling method to address the issues of low strength and weak lifting effect of steel wire ropes and constructed a BP neural network to extract multiple sets of time-domain feature values as inputs for feature recognition [15]. Nevertheless, conventional manual feature extraction methods necessitate a substantial amount of prior expertise to process and analyze the original signal, and the extraction and selection of signal features are subject to limitations.

As the advent of deep learning has occurred, artificial intelligence-based deep learning theories have begun to be utilized for the non-destructive detection of broken wire damage in steel wire ropes. Deep learning harnesses self-supervised reverse algorithms for optimization and adjustment, enabling the automatic extraction of fault feature information from the original signal devoid of manual interference. It sequentially processes this information layer by layer, transforming it into abstract features conducive to classification. Consequently, it mitigates the constraints linked to manual feature selection [16,17]. Zhang et al. proposed a quantitative recognition model based on convolutional neural networks to address the issue of insufficient manual signal feature extraction, converting one-dimensional signals into two-dimensional signals and thereby improving the accuracy and speed of wire rope breakage recognition [18]. Huang et al. used machine vision technology to train ground wave radar surface images, automatically extract discriminative features, and import them into the constructed convolutional neural network for training, overcoming the inherent limitations of manual feature extraction methods and achieving good results [2].

However, it is worth noting that the above-mentioned wire breakage detection methods mainly focus on detecting external wire breakage damage, and there has been relatively limited research on the detection of internal wire breakage damage characteristics. Therefore, there is an urgent need for a new method to accurately identify the internal and external wire breakage characteristics of steel wire ropes. The residual network was proposed by Microsoft Labs in 2015; it greatly improves the training depth and speed of the network and enhances its feature extraction ability by utilizing residual modules. Hence, residual networks will be proposed and compared with three common neural networks in this article, using sample data to adjust network parameters in a timely manner and determine the optimal method for quantitative damage identification.

The main research findings of this article are as follows:

1. A new method for processing broken wire signals has been proposed, which converts the one-dimensional signal of broken wire MFL into a two-dimensional time–

frequency map through a neural network, eliminating the tedious step of manually extracting features and improving the efficiency of signal processing.

- By constructing a residual network for internal wire breakage recognition and utilizing the residual module to improve the training depth and speed of the network, the accuracy of identifying internal wire breakage within steel wire ropes can be markedly enhanced.

The rest of this article is organized as follows: Section 2 introduces the theoretical knowledge of convolutional neural networks and residual networks. Section 3 provides detailed preparations for the experiment. In Section 4, the experimental method of this paper is proposed, and the accuracy of four neural networks for wire breakage recognition is compared. Finally, the conclusions are drawn in Section 5.

2. Theoretical Background

2.1. Convolutional Neural Network

A convolutional neural network (CNN) is a multi-layer feedforward neural network structure that mainly consists of input layers, convolutional layers, pooling layers, fully connected layers, and output layers [19]. The structure of a convolutional neural network is illustrated in Figure 1. The convolutional and pooling layers are arranged alternately, and the results are finally output through one or more fully connected layers. Additionally, loss functions, batch normalization, and other operations are added to the CNN structure to optimize its performance.

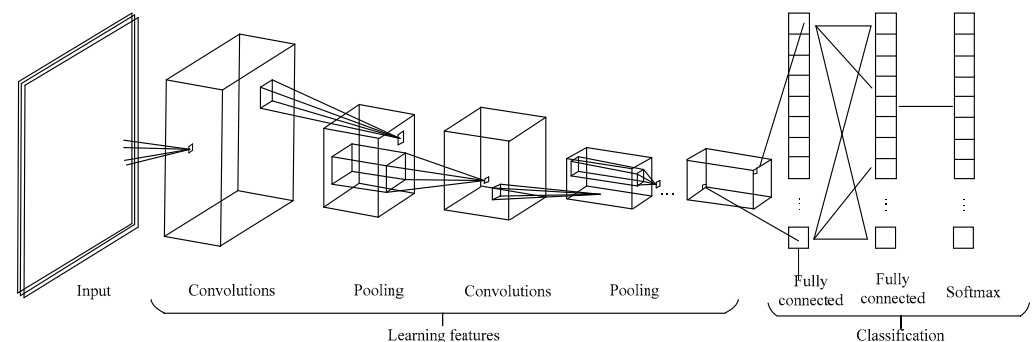


Figure 1. Convolutional neural network framework.

The convolutional layer is the core of convolutional neural networks and mainly extracts autonomous feature information through convolutional kernels. By adjusting the size and stride of the convolutional kernels, the transformation from input to output can be controlled. The parameters and bias values of the convolutional kernels in convolutional neural networks are typically initialized randomly [20]. During the training process, these parameters and bias values are updated through backpropagation. In the convolutional layer, multiple convolutional kernels are used to convolve the input image data. After the addition of bias, a series of feature maps are obtained through an activation function [20]. The convolution process can be calculated as follows:

$$x_j^l = f\left(\sum_{i \in M_j} x_i^{l-1} * k_{ij}^l + b_j^l\right) \quad (1)$$

where the M_j represents the j -th convolutional region of the input feature map; x_i^{l-1} is the i -th element of the $(l-1)$ -th layer in the network, and k is the matrix of the convolution kernel; f is a nonlinear activation function; b_j^l represents the bias of the output feature map.

The pooling layer compresses the data volume through down-sampling, increasing the receptive field. Usually, two methods, mean pooling and maximum pooling, are used for pooling processing. After several alternating convolution and pooling layers, one or more fully connected layers are usually connected to achieve intelligent classification and recognition.

2.2. Residual Network

The residual network was proposed by Microsoft Labs in 2015, and its advantage lies in the introduction of the residual module [21]. The depth of a model impacts the intricacy of the extracted features and the quantity of model parameters. Nevertheless, deeper models are susceptible to challenges such as gradient explosion or vanishing. The residual network addresses this issue by employing the residual module [22,23]. This approach significantly improves the training depth and speed of the network while enhancing its feature extraction capability. There are several types of residual networks, such as ResNet18, ResNet50, and ResNet101. Numbers represent the number of layers in the residual network. ResNet18 has a moderate number of layers and fast training speed and belongs to the deep separable CNN architecture, which is widely used in classification tasks. In response to the relatively small scale and high real-time requirements of wire rope breakage damage classification tasks, this paper selects ResNet18 as the main network model, and its structural model is shown in Figure 2.

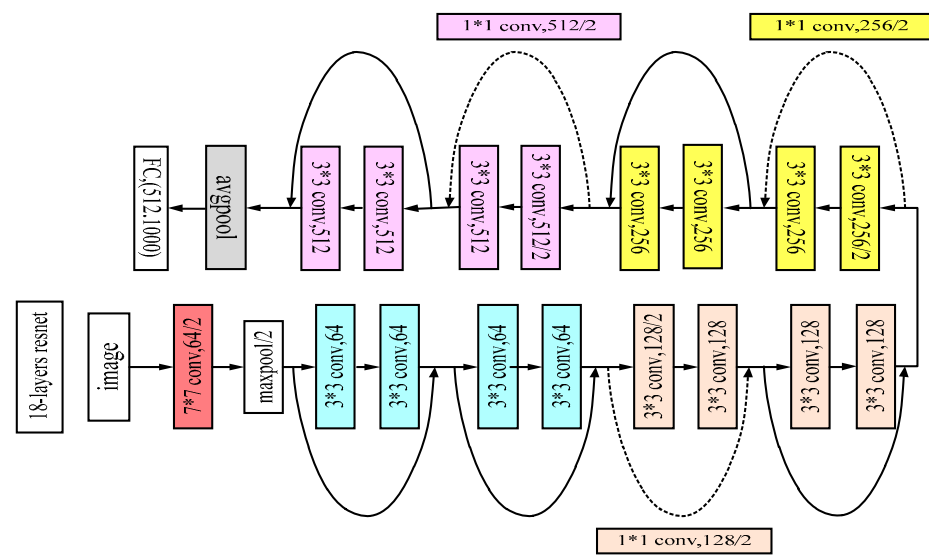


Figure 2. Residual network.

The ResNet18 architecture begins by performing convolution calculations on a two-dimensional RGB image with three channels and an input size of $224 \times 224 \times 3$. Then, four residual modules are used, each consisting of two convolutional layers and a skip connection. The four residual modules are stacked twice and finally inputted into a fully connected layer. The extracted broken wire damage features are used to predict the probability of classification results through a SoftMax classifier. Figure 3 illustrates the structure of the first residual module (residual module I) in ResNet18. This module starts with a 3×3 convolution operation with 64 channels, followed by batch normalization and the ReLU activation function to enhance the network's convergence speed. The output of this operation is then added to the input feature map using the ReLU activation function. This process is repeated once, resulting in a convolution size of $56 \times 56 \times 64$. This is followed by the convolution of the second residual module, whose residual module II is shown in Figure 4. The second residual module uses a 128-channel convolution kernel with a size of 28×28 . In order to add to the output feature map of the previous residual module, a $1 \times 1 \times 128$ convolution needs to be added to the skip connection for up-sampling and down-sampling. The skip connection can directly connect the input to the output, allowing the network to learn residual information and better perform feature extraction and processing. The ability of residual networks to learn identity maps is mathematically represented by the following function:

$$F(x) = H(x) - x \quad (2)$$

where the x represents the input vector of the neural network, $F(x)$ represents the residual mapping that needs to be learned, $F(x)$ adds the corresponding elements to x , and the expected output vector is $H(x)$. When $F(x) = 0$, an identity mapping can be formed.

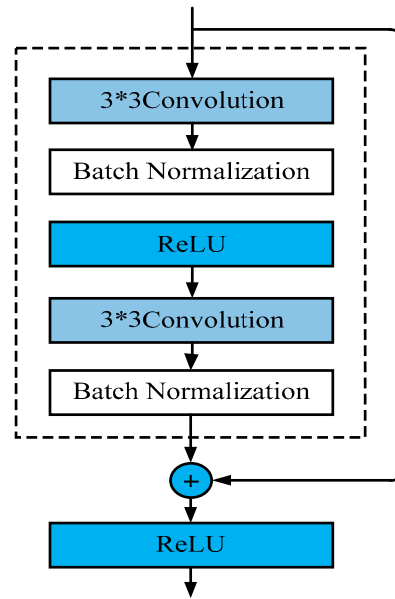


Figure 3. Basic structure of residual module I.

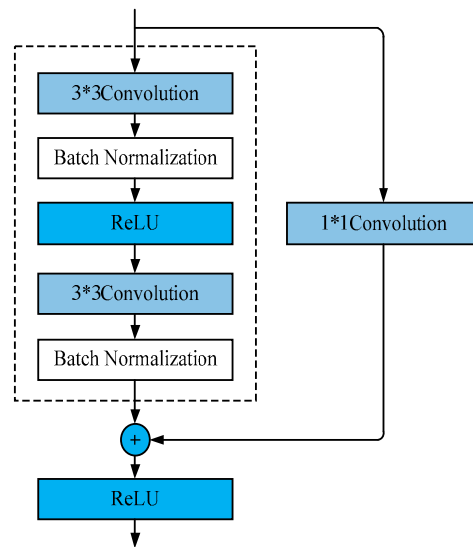


Figure 4. Basic structure of residual module II.

3. Experimental Study

3.1. Sample Production

To simulate real working conditions, a total of 18 types of internal and external broken wire specimens were created for galvanized steel wire ropes with diameters of 20 mm, 22 mm, and 24 mm. For each diameter, there were 1–3 external broken wires and 1–3 internal broken wires. The corresponding labels and fault descriptions can be found in Table 1. The fracture length of the broken wire is 12 mm. As an example, Figure 5 illustrates the 6 types of broken wire specimens present both inside and outside the 20 mm diameter steel wire rope.

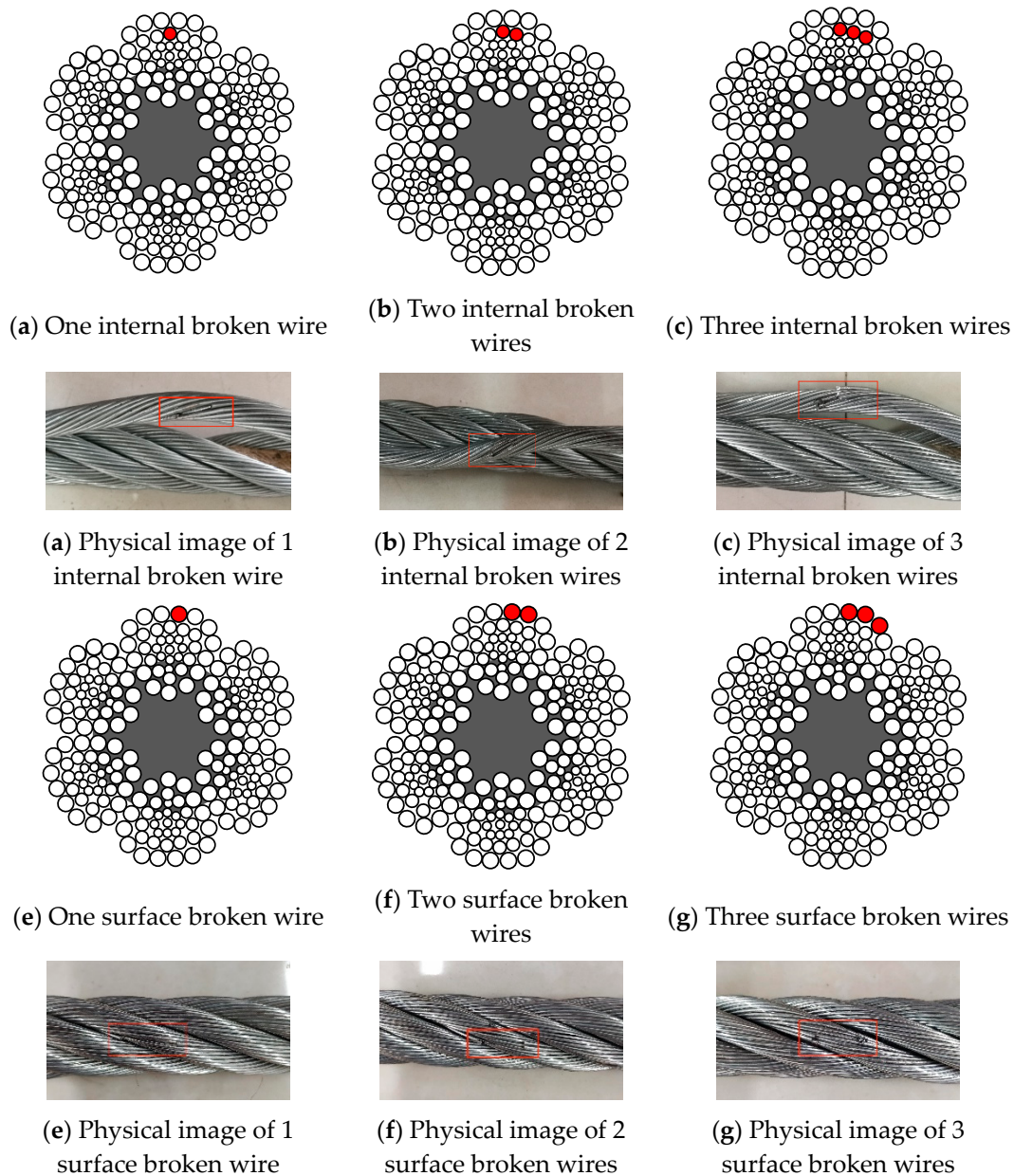


Figure 5. Physical images of broken wire test pieces.

Table 1. Broken wire label.

Label	Description (Diameter 20 mm)	Label	Description (Diameter 22 mm)	Label	Description (Diameter 24 mm)
1	1 internal broken wire	7	1 internal broken wire	13	1 internal broken wire
2	2 internal broken wires	8	2 internal broken wires	14	2 internal broken wires
3	3 internal broken wires	9	3 internal broken wires	15	3 internal broken wires
4	1 surface broken wire	10	1 surface broken wire	16	1 surface broken wire
5	2 surface broken wires	11	2 surface broken wires	17	2 surface broken wires
6	3 surface broken wires	12	3 surface broken wires	18	3 surface broken wires

3.2. Signal Extraction

The wire rope breakage and damage detection test bench is illustrated in Figure 6a. Rope buckles are created at both ends of the wire rope with broken wires and damage, and the wire rope is securely fastened to the test bench using the rope buckle. During the signal acquisition process, the tray is controlled to move along the guide rail, driving the sensor in the direction of the steel wire rope for damage detection. The sensor preprocesses the magnetic leakage signal collected by the circuit board and transmits it to the signal acquisition system. Figure 6b shows the signal acquisition system, which utilizes NI and LabVIEW to achieve real-time display and storage of the signal. Figure 7 shows the one-dimensional magnetic leakage signal of the steel wire rope collected by the focusing magnetic sensor.

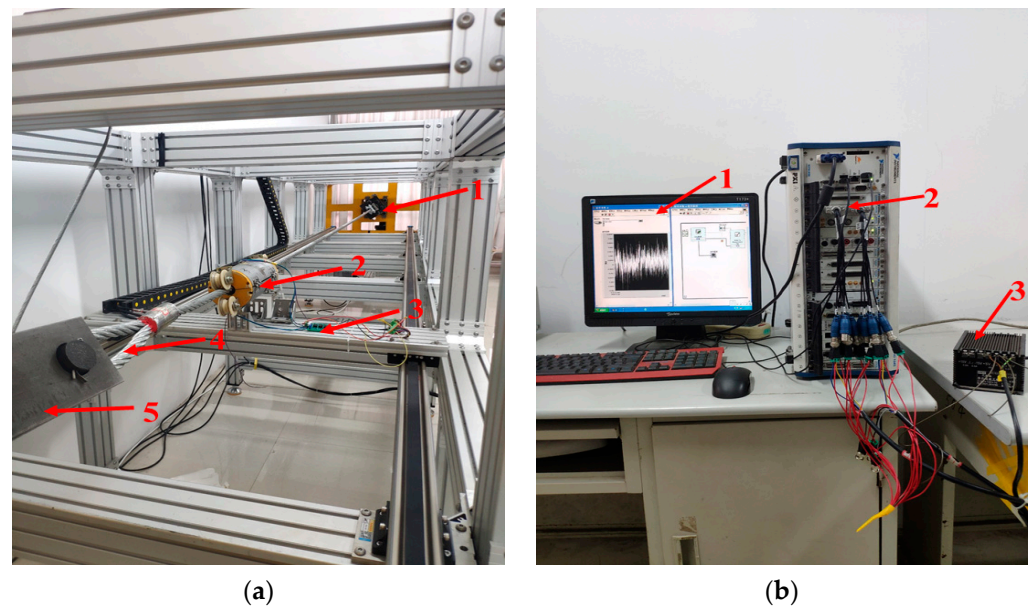


Figure 6. (a) Steel wire rope inspection test bench: 1—loading device; 2—detector; 3—movable tray; 4—cord lock; 5—fixing pin. (b) Signal acquisition system: 1—LabVIEW program; 2—NI 4496 card; 3—DC power supply.

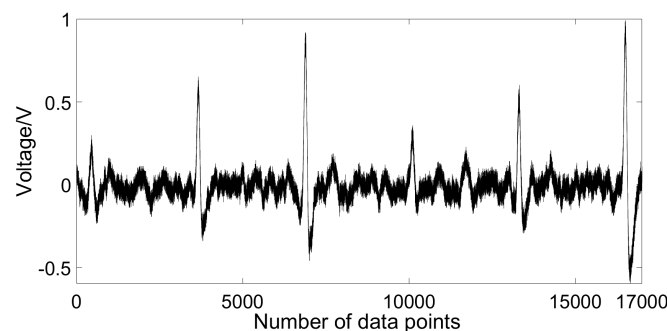


Figure 7. The one-dimensional raw signal collected by the MFL sensor.

3.3. Time–Frequency Conversion

The signal collected by the MFL sensor is a one-dimensional MFL signal. To better suit convolutional neural networks and residual network models, it is necessary to convert the one-dimensional MFL signal into a two-dimensional time–frequency image using time–frequency analysis technology. This article utilizes continuous wavelet transform (CWT) to extract time-domain and frequency-domain features of MFL signals. These features are

then used as inputs for quantitative identification in neural networks. The continuous wavelet transform of signal $f(t)$ can be expressed as follows:

$$CWT_f(u, s) = \langle f(t), \psi_{u,s}(t) \rangle = \int_{-\infty}^{+\infty} f(t) \frac{1}{\sqrt{s}} \psi^* \left(\frac{t-u}{s} \right) dt \quad (3)$$

where wavelet time–frequency atoms $\psi_{u,s}(t) = \frac{1}{\sqrt{s}} \psi \left(\frac{t-u}{s} \right)$ are obtained by scaling (s : scale factor) and translating (u : shift factor) the mother wavelet. After the wavelet transform, the one-dimensional signals $f(t)$ are decomposed into a series of wavelet coefficients related to scale and translation factors, which are then projected into a two-dimensional time–frequency distribution image.

Taking the inner and outer damage samples of a 20 mm diameter steel wire rope as an example, the time–frequency images obtained through continuous wavelet transform (CWT) are shown in Figure 8. The horizontal axis in the picture represents the time domain, and the vertical axis represents the frequency domain.

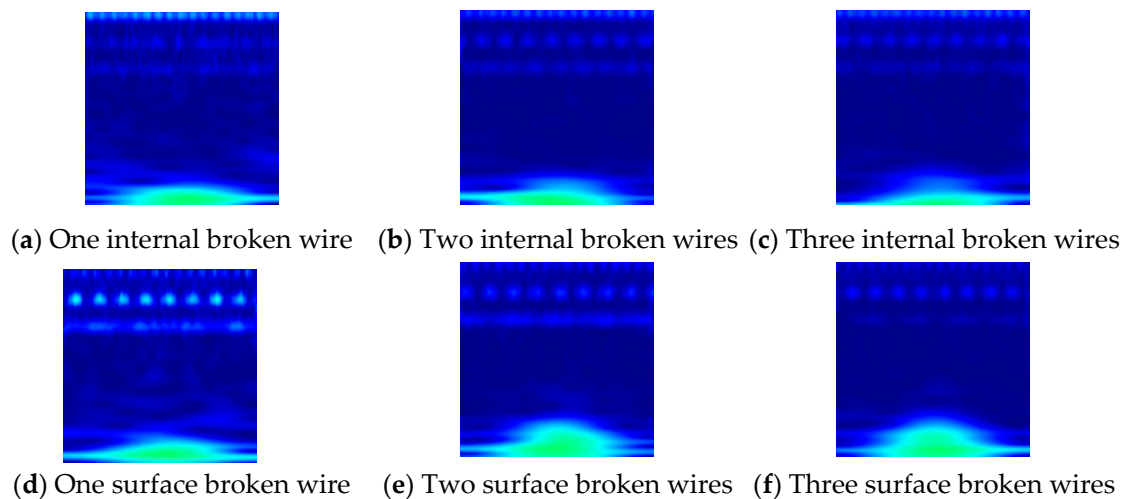


Figure 8. Time–frequency diagram of internal and external wire breakage of 20 mm diameter steel wire rope.

4. Experimental Results

4.1. Experimental Procedure

In order to verify the recognition effect of internal wire breakage in steel wire ropes using residual networks, this paper conducts comparative experiments and compares the residual network with three other neural networks. The basic framework is shown in Figure 9. Firstly, this article uses continuous wavelet transform technology to convert one-dimensional MFL signals into two-dimensional time–frequency maps, preserving the time-domain and frequency-domain information of the signals, and constructs a Residual Network 18 (ResNet18) model. The preprocessed time–frequency characteristics are used as inputs to ResNet18. Secondly, as a comparison, a convolutional neural network is constructed, and the two-dimensional time–frequency map transformed by continuous wavelet transform is used as the input of the convolutional neural network. Feature vectors formed by the peak, pulse width, and inter-peak features are manually extracted from the signal, and the backpropagation (BP) neural network and the support vector machine (SVM) are constructed, with the manually extracted signal features being used as inputs for quantitative recognition in the latter two networks. Finally, the article will compare the accuracy of internal and external disconnection for the four models and select the best recognition model.

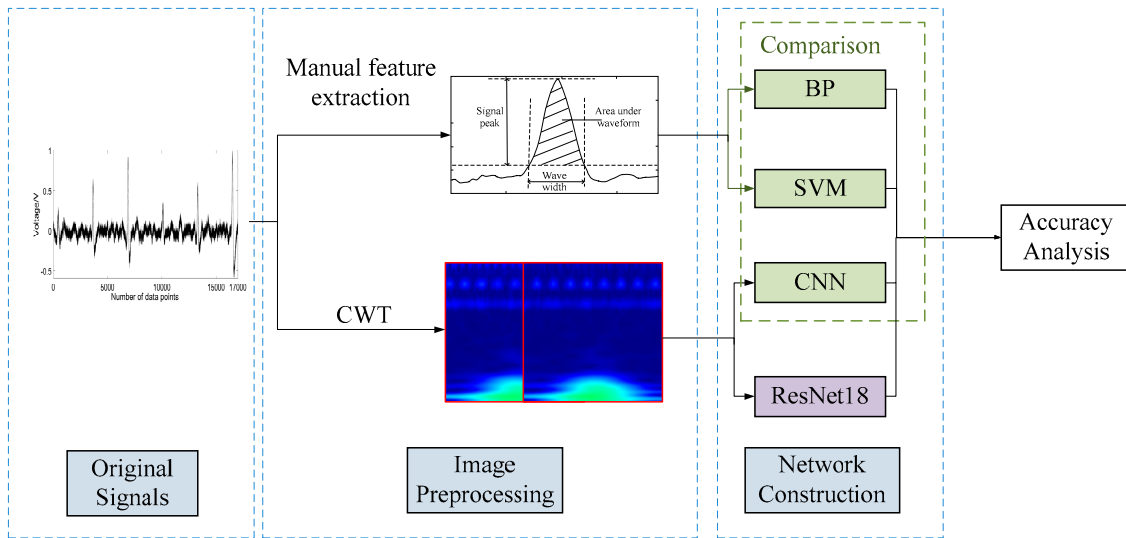


Figure 9. The framework of the experimental method.

4.2. Analysis of Residual Network Model Results

After the one-dimensional MFL signals of 18 types of internal and external broken wires in steel wire ropes with diameters of 20 mm, 22 mm, and 24 mm are converted into two-dimensional time–frequency maps of size 224×224 through continuous wavelet transform (CWT), a total of 1800 image sample data are obtained; 75% of the sample data is used for network training, and the remaining 25% is used for testing the network. The network structure of ResNet18 consists of an input layer, four residual modules, a fully connected layer, and an output layer, effectively addressing gradient vanishing and exploding issues through the use of residual modules. The network is initialized with a learning rate of 0.0015, and each iteration utilizes 30 training subsets. The training progress is visualized by plotting the training progress, and the recognition accuracy results are shown in Figure 10. The quantitative recognition method for broken wires in steel wire ropes based on ResNet18 can accurately identify the internal and external broken wire faults of steel wire ropes. The overall recognition accuracy reaches 95.33%, which is 6.66% higher than that of convolutional neural networks, providing a reliable basis for identifying damage to steel wire ropes.

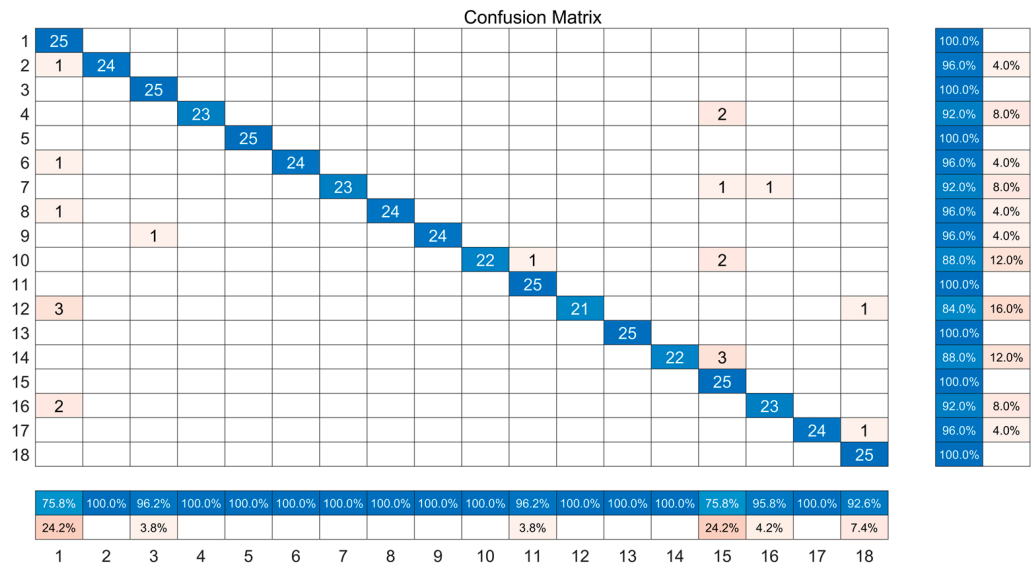


Figure 10. The confusion matrix based on ResNet18.

fewer hyperparameters and exhibits strong classification ability, has shown good results in identifying broken wire damage in steel wire ropes. In this study, cross-validation was used to set the learning parameter misclassification penalty factor C to 0.1 and the parameter Gamma of the radial basis function to 5. The one-dimensional signal collected by the sensor was manually extracted with damage features such as the peak and width, and this feature information was used as inputs for the support vector machine model for quantitative recognition. The confusion matrix, shown in Figure 12, indicates that the accuracy of the support vector machine classification model is 64.81%.

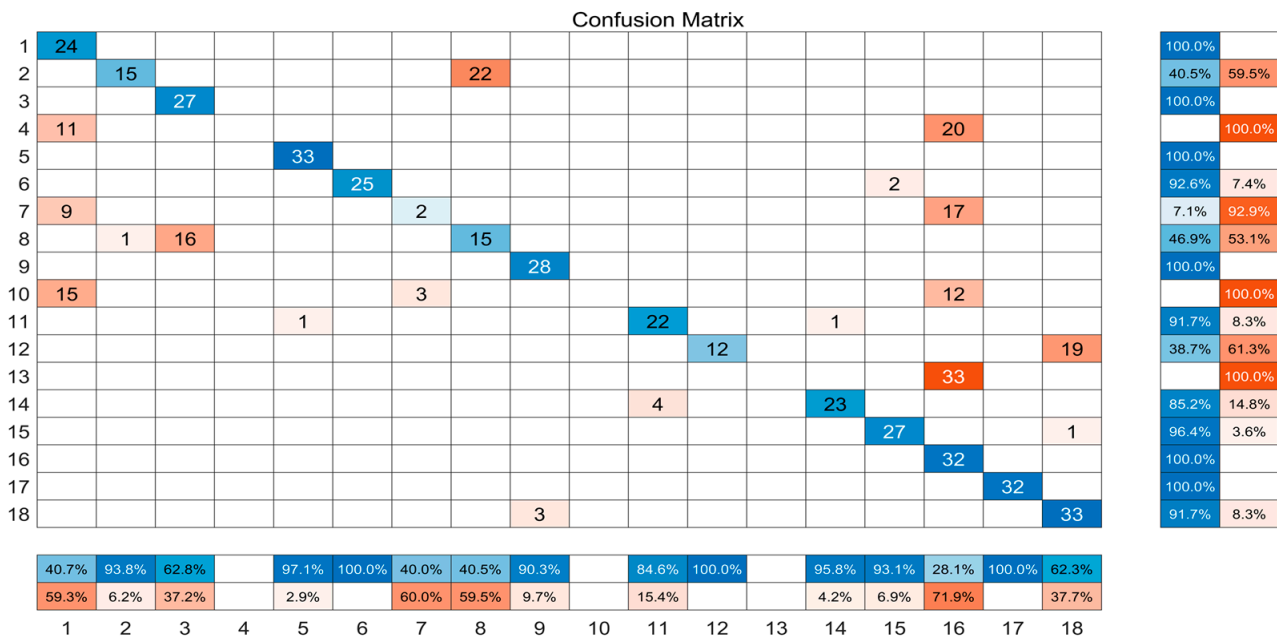


Figure 12. The confusion matrix based on SVM.

4.5. Analysis of Convolutional Neural Network Model Results

This study conducted a comprehensive analysis of the one-dimensional magnetic leakage signals of 18 types of internal and external broken wires in steel wire ropes with diameters of 20 mm, 22 mm, and 24 mm. The signals were transformed into two-dimensional time–frequency maps using continuous wavelet transform (CWT), resulting in a total of 1800 image sample data of size 227 × 227. The network training utilized 75% of the sample data, while the remaining 25% was used for testing. The convolutional neural network was trained with an iteration epoch number of 5, and the solving environment was set to CPU. The network structure consisted of three convolutional layers, two max pooling layers with a step size of 2, and an output layer for classifying the 18 types of broken wire faults. After each convolution, a normalization layer and ReLU activation function were applied. The classification results were visualized using a confusion matrix, which is shown in Figure 13. The convolutional neural network achieves a final accuracy of 88.44% with an error rate of 11.56%, with particular shortcomings observed in the recognition performance of the third and fourth broken wire features. Notably, the overall recognition accuracy of the convolutional neural network was superior to that of traditional BP neural networks and support vector machines.

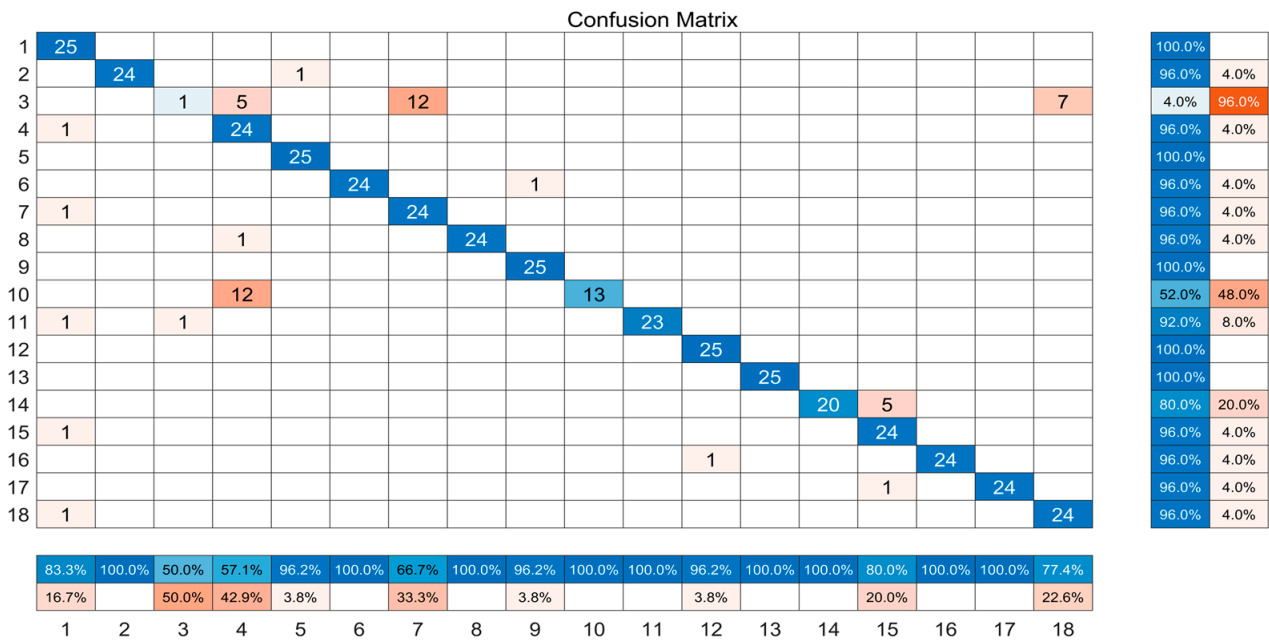


Figure 13. The confusion matrix based on convolutional neural network.

4.6. Overall Evaluation Indicators

In order to evaluate the effectiveness of various neural network models in the classification of steel wire rope damage faults, relying solely on the confusion matrix to evaluate the model quality is relatively singular. Therefore, this paper introduces the overall classification accuracy (OA coefficient) and Kappa coefficient evaluation indicators to judge the classification accuracy. The OA coefficient represents the value obtained by comparing the number of correctly classified pixels to the total number of labeled pixels. The Kappa coefficient is based on the confusion matrix and is used to measure the consistency between evaluators. Its value range is in the interval [-1,1], and the closer the value is to 1, the higher the consistency of the evaluation. The OA coefficient and Kappa coefficient calculation formula based on a confusion matrix are as follows:

$$OA = \frac{\sum_{i=1}^n h_{ii}}{\sum_{i=1}^n N_i} \tag{4}$$

where N is the number of categories of the image target, N_i is the number of $i - th$ class pixels, and h_{ii} is the number of correctly classified $i - th$ class pixels.

$$M = \begin{pmatrix} m_{11} & \dots & m_{1N_r} \\ \vdots & \ddots & \vdots \\ m_{N_r1} & \dots & m_{N_rN_r} \end{pmatrix} \tag{5}$$

$$Kappa = \frac{N \sum_{i=1}^N m_{ii} - \sum_{i=1}^N m_i + m_{+i}}{N^2 - \sum_{i=1}^N m_i + m_{+i}} \tag{6}$$

where the M represents the confusion matrix and m_{ij} represents the number of pixels in class i that have been misclassified into class j . If the values of i and j are the same, they represent the number of correctly classified samples, while if i and j are different, they represent the number of misclassified samples. The calculation method of the Kappa

coefficient is shown in Equation (6), where N is the number of pixels tested in the total training sample and “+” refers to the sum that can be performed on rows or columns.

The classification results of the four neural network models are shown in Table 2, where the horizontal axis represents the four prebuilt neural network models, and the vertical axis represents the evaluation indicators using OA and Kappa coefficients. Figure 14 presents the accuracy of four neural network classification results in a more intuitive manner using a bar chart format. From Figure 13, it can be seen that the residual network has higher OA and Kappa coefficients, which are more suitable for wire rope fault classification and have achieved good classification results.

Table 2. Statistical table of classification results.

Evaluation Indicator	BP Neural Network	SVM	CNN	ResNet18
OA coefficient	36.43%	64.70%	88.44%	94.29%
Kappa coefficient	32.61%	62.62%	87.76%	93.95%

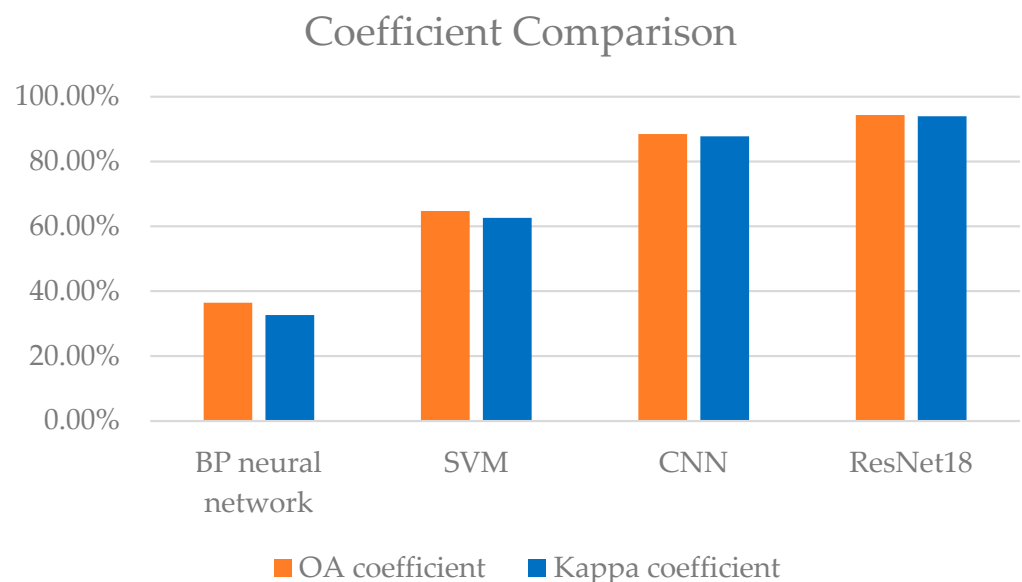


Figure 14. Comparison chart of classification results.

4.7. Comparison of Visualization Results

In order to better compare the recognition performance of the prebuilt neural networks, the T-SNE algorithm was used to visualize the recognition features of four classification models: backpropagation neural network, support vector machine (SVM) classification model, convolutional neural network (CNN), and deep residual network (ResNet18), as shown in Figure 15. The depicted figure distinctly showcases that the residual network, following meticulous layer-by-layer processing, facilitates precise discrimination among 18 distinct types of damage features, outperforming the classification efficacy of the remaining three models.

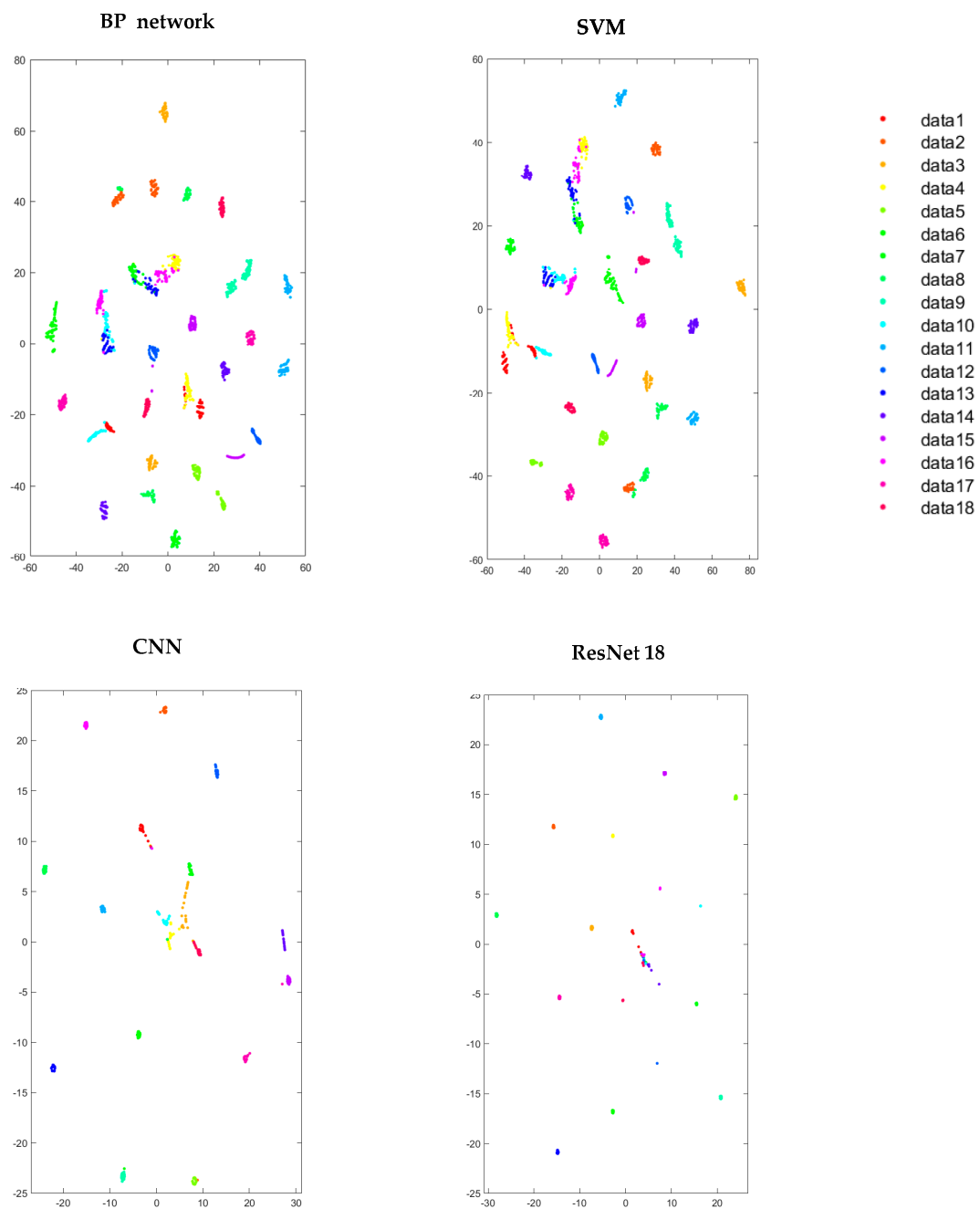


Figure 15. Feature dimension reduction results by using T-SNE.

5. Conclusions

This article aims to identify the types of broken wire damage in steel wire ropes more quickly and accurately and proposes a method for identifying internal and external broken wire damage in steel wire ropes based on ResNet18. The ResNet18 network has a moderate number of layers and fast convergence speed, which is suitable for the classification task of broken wire damage in steel wire ropes with relatively small scale and high real-time requirements. Comparing the accuracy of traditional neural networks and deep learning networks, the results show that the recognition rates of the two traditional neural networks are relatively low, while deep learning networks have higher recognition accuracy. Specifically, the ResNet18 network has an accuracy of 95.33%, which is conducive to improving the effectiveness of wire breakage recognition. We compared the recognition accuracy of the four classification models using four evaluation indicators: confusion matrix,

recognition feature visualization, overall classification accuracy, and Kappa coefficient. The results indicate that the ResNet model is more accurate compared to other models and has good application prospects.

Although the proposed ResNet18 model demonstrates excellent performance in classifying external and internal wire breakages on the steel ropes, it has only been tested under laboratory conditions. Currently, we are simulating real experimental conditions and conducting a large number of testing experiments, striving to make the data collection and testing accuracy of wire rope damage closer to real conditions.

Author Contributions: Conceptualization, J.H. and Y.Z.; methodology, J.H.; software, Z.F.; validation, J.H. and L.Z.; formal analysis, J.H.; investigation, Z.F.; resources, Y.Z.; data curation, J.H.; writing—original draft preparation, J.H.; writing—review and editing, Y.Z.; visualization, Z.F.; supervision, Y.Z.; project administration, L.Z.; funding acquisition, L.Z. All authors have read and agreed to the published version of the manuscript.

Funding: This research was funded by Doctoral Start-up Funds (No. 318052148).

Institutional Review Board Statement: Not applicable.

Informed Consent Statement: Not applicable.

Data Availability Statement: The raw data supporting the conclusions of this article will be made available by the authors on request.

Conflicts of Interest: The authors declare no conflicts of interest.

References

1. Chen, H.; Guo, L.; Liu, H.; Chen, H. Finite element study of behaviour and interface force conditions of locked coil wire rope under axial loading. *Constr. Build. Mater.* **2021**, *272*, 121961. [[CrossRef](#)]
2. Huang, X.; Liu, Z.; Zhang, X.; Kang, J.; Zhang, M.; Guo, Y. Surface damage detection for steel wire ropes using deep learning and computer vision techniques. *J. Meas.* **2020**, *161*, 107843. [[CrossRef](#)]
3. Zhou, P.; Zhou, G.; Zhu, Z.; He, Z.; Ding, X.; Tang, C. A Review of Non-Destructive Damage Detection Methods for Steel Wire Ropes. *J. Appl. Sci.* **2019**, *9*, 2771. [[CrossRef](#)]
4. Wang, H.; Tian, J.; Tian, Z. Simulation analysis and experimental investigation of wire rope leakage magnetic field detection. *Insight* **2023**, *65*, 203–208. [[CrossRef](#)]
5. Li, X.; Zhang, X.; Shi, J. Quantitative Nondestructive Testing of Broken Wires for Wire Rope Based on Magnetic and Infrared Information. *J. Sens.* **2020**, *2020*, 6419371. [[CrossRef](#)]
6. Raisutis, R.; Kažys, R.; Mažeika, L.; Žukauskas, E.; Samaitis, V.; Jankauskas, A. Ultrasonic guided wave-based testing technique for inspection of multi-wire rope structures. *NDT E Int.* **2014**, *62*, 40–49. [[CrossRef](#)]
7. Kresak, J.; Peterka, P.; Kropuch, S.; Novák, L. Measurement of tight in steel ropes by a mean of thermovision. *Measurement* **2014**, *50*, 93–98. [[CrossRef](#)]
8. Weischedel, H.R. *The Magnetic Flux Leakage Inspection of Wire Ropes*; NDT Technologies, Inc.: Montreal, QC, Canada, 2009; pp. 1–19.
9. Yan, X.; Zhang, D.; Pan, S.; Zhang, E.; Gao, W. Online nondestructive testing for fine steel wire rope in electromagnetic interference environment. *NDT E Int.* **2017**, *92*, 75–81. [[CrossRef](#)]
10. Liu, S.; Sun, Y.; Jiang, X.; Kang, Y. Comparison and analysis of multiple signal processing methods in steel wire rope defect detection by hall sensor. *J. Meas.* **2021**, *171*, 108768. [[CrossRef](#)]
11. Tian, J.; Wang, H.; Zhou, J.; Meng, G. Study of pre-processing model of coal-mine hoist wire-rope fatigue damage signal. *J. Min. Sci. Technol.* **2015**, *25*, 1007–1011. [[CrossRef](#)]
12. Kim, J.W.; Tola, K.D.; Tran, D.Q.; Park, S. MFL-Based Local Damage Diagnosis and SVM-Based Damage Type Classification for Wire Rope NDE. *Materials* **2019**, *12*, 2894. [[CrossRef](#)] [[PubMed](#)]
13. Mukhopadhyay, S.; Srivastava, G.P. Characterisation of metal loss defects from magnetic flux leakage signals with discrete wavelet transform. *NDT E Int.* **2000**, *33*, 57–65. [[CrossRef](#)]
14. Qin, Y.; Hua, X.; Lian, M. Wire Rope Fault Diagnosis Based on Wavelet Analysis and Support Vector Machine (SVM). *Adv. Mater. Res.* **2014**, 971–973, 1396–1399. [[CrossRef](#)]
15. Zhou, C.; Wei, C.; Wang, W. A New Detection Method Based on Magnetic Leakage Theory and BP Neural Network for Broken Steel Strands in ACSR Conductor. *IEEE Sens. J.* **2022**, *22*, 19620–19634. [[CrossRef](#)]
16. Huang, W.; Cheng, J.; Yang, Y. An improved deep convolutional neural network with multi-scale information for bearing fault diagnosis. *J. Neurocomput.* **2019**, *359*, 77–92. [[CrossRef](#)]
17. Gündüz, H.A.; Binder, M.; To, X.Y.; Mreches, R.; Bischl, B.; McHardy, A.C.; Münch, P.C.; Rezaei, M. A self-supervised deep learning method for data-efficient training in genomics. *Commun. Biol.* **2023**, *6*, 928. [[CrossRef](#)] [[PubMed](#)]

18. Zhang, Y.; Feng, Z.; Sheng, S. A quantitative identification method based on CWT and CNN for external and inner broken wires of steel wire ropes. *Heliyon* **2022**, *8*, e11623. [[CrossRef](#)] [[PubMed](#)]
19. Chen, X. The Study for Convolutional Neural Network and Corresponding Applications. *Null* **2023**, *5*, 182–187. [[CrossRef](#)]
20. Tang, S.; Yuan, S.; Zhu, Y. Convolutional neural network in intelligent fault diagnosis toward rotatory machinery. *IEEE Access* **2020**, *8*, 86510–86519. [[CrossRef](#)]
21. He, K.; Zhang, X.; Ren, S. Deep residual learning for image recognition. In Proceedings of the IEEE Conference on Computer Vision and Pattern Recognition, Las Vegas, NV, USA, 27–30 June 2016; pp. 770–778.
22. Fang, J.; Lin, X.; Tian, J.; Wu, Y. Face recognition technology in classroom environment based on ResNet neural network. *Electron. Imaging* **2022**, *31*, 051421. [[CrossRef](#)]
23. Xie, L.; Huang, C. A Residual Network of Water Scene Recognition Based on Optimized Inception Module and Convolutional Block Attention Module. In Proceedings of the 2019 6th International Conference on Systems and Informatics, Shanghai, China, 2–4 November 2019.

Disclaimer/Publisher’s Note: The statements, opinions and data contained in all publications are solely those of the individual author(s) and contributor(s) and not of MDPI and/or the editor(s). MDPI and/or the editor(s) disclaim responsibility for any injury to people or property resulting from any ideas, methods, instructions or products referred to in the content.